Journal of Petroleum Science and Engineering 217 (2022) 110919

Contents lists available at ScienceDirect

Journal of Petroleum Science and Engineering

journal homepage: www.elsevier.com/locate/petrol

Source rock evaluation and petroleum generation of the Lower Cretaceous Yamama Formation: Its ability to contribute to generating and expelling petroleum to cretaceous reservoirs of the Mesopotamian Basin, Iraq

Amer Jassim Al-Khafaji [a,*], Fahad M. Al-Najm [b], Rana A.K. Al-Refaia [c], Fadhil N. Sadooni [d], Mohanad R.A. Al-Owaidi [a], Hamid A. Al-Sultan [a]

[a] Department of Geology, College of Science, University of Babylon, Al Ḥillah, Iraq
[b] Department of Geology, College of Science, University of Basrah, Basra, Iraq
[c] Department of Chemistry, College of Science, University of Babylon, Al Ḥillah, Iraq
[d] Environmental Science Center, Qatar University, Doha, Qatar

ARTICLE INFO

Keywords:
Yamama source rocks
Palynofacies
Organic geochemistry
Basin modeling
Oil generation
Mesopotamian basin
South Iraq

ABSTRACT

The Yamama Formation is an important reservoir as well as a good source rocks in many of the oilfields of the southern Mesopotamian Basin, Iraq. The formation represents a regressive cycle deposited in a shallow carbonate ramp that was under clastic influence from the nearby land. This setting is a determining factor in the organic matter content. Geochemical pyrolysis, palynofacies, biomarkers, and carbon isotope analyses were conducted on 152 samples from 27 oil wells. The formation represents a regressive cycle deposited in a shallow carbonate ramp that was under clastic influence from the nearby land. Based on pyrolysis analyses, the source rocks have poor to excellent hydrocarbon potential. The kerogen types of the Yamama source are varied, including II, II/III, III, and I. This is due to the varied depositional environments and related organic matter sources (continental to marine).

The studied samples also showed a variety in distribution between oil-prone kerogen type II, distal sub-oxic–anoxic and the dysoxic–anoxic marine carbonate environments of (IX) and (VIII) zones of Tyson Ternary, which reflect the wide variations in the sediment depositional paleo-environments. The difference in the variations of normal alkanes of light alkanes in the range of n-C13 to n-C19 of the gas chromatography analyses, as well as the verities of the biomarker ratio of the tricyclic terpanes, hopane, and homohopane, indicate differences in the depositional setting. Similarly, the carbon stable isotope compositions of ^{13}C (‰) saturated and ^{13}C (‰) aromatic hydrocarbons, as well as the canonical variable value for Yamama source rock extracts, correspond to a variety of organic matter sources, ranging from open marine to terrestrial with plants.

The Tmax values for most Yamama source samples range from 430 °C to 451 °C, the C_{27} Ts/Tm, C_{29} sterane 20S/(20 S + 20 R) and ββ/(ββ+αα) stereoisomer, and triaromatic steroids 3 [TAS3]) ratios, indicating that the studied samples are in the range "immature to oil window", and that Tmax of 430–450 °C corresponds to an early to peak oil window stage. The Yamama source intervals entered the early oil window in the Late Cretaceous ranging from 80 to 62 Ma and completed oil generation in the early Eocene to Late Miocene approximately 80 to 62 Ma, according to 1D-Burial, thermal history modeling, and the timing of oil generation of selected wells covering the studied area (58–7 Ma). This confirms that these source intervals have completed petroleum generation and have contributed significantly to the supplies of crude oil and gas to surrounding reservoirs.

1. Introduction

The Yamama Formation of Valanginian age was introduced to the Arabian stratigraphy by (Steinke and Bramkamp, 1952) in Saudi Arabia to be distinguished from the Ratawi Formation. By extension, the formation name has been applied to the upper part of a more or less continuous pellety limestone sequence which underlies the shaly Ratawi Formation in the Ratawi well of southern Iraq, and also Burgan 113 in

* Corresponding author.
E-mail address: a.alkhafaji@uobabylon.edu.iq (A.J. Al-Khafaji).

https://doi.org/10.1016/j.petrol.2022.110919
Received 25 January 2021; Received in revised form 13 January 2022; Accepted 22 July 2022
Available online 10 August 2022

Kuwait. In southern Iraq, the Yamama Formation is one of the most major Lower Cretaceous carbonate reservoirs. At the same time, the Formation contains important source rocks that may be responsible for the generation of some of the oil stored in the Cretaceous reservoirs in the area, (Fig. 1); (Sadooni, 1993).

The Yamama Formation is formed of shallow water carbonates containing large benthonic foraminifera, red and green algae with some horizons of oolitic packstone and grainstone. The Yamama carbonates grade upward into the shale and fine sand of the Ratawi Formation, which is considered as the caprock of the Yamama reservoir units. The Yamama Formation is underneath by the Upper Jurassic to Lower Cretaceous Sulaiy Formation which consists mainly of sub-basinal chalky and argillaceous limestone. The Jurassic-Cretaceous boundary in southern Iraq passes through the upper part of this Formation, (Sadooni, 2018), Fig. 2 (see Fig. 3).

Jurassic-early Cretaceous in Iraq, Kuwait, and Saudi Arabia. Modified after (Sharland et al., 2011).

The Yamama source potential have been investigated by many workers such as ((Al-Marsoumi et al., 2005); (Abeed et al., 2011); (Abeed et al., 2013); (Ahmed and Al Obaidi, 2018) ((Al-Ameri and Ai-Khafaji, 2014); (Al-Khafaji, 2015); (Al-Khafaji et al., 2019a), (Al-Khafaji et al., 2019b), (Al-Khafaji et al., 2020), (Al-Khafaji et al., 2021)). They concluded that the Yamama source rocks were deposited in alternating suboxic to anoxic depositional conditions basin and that they have very good hydrocarbons indices with moderate to higher levels of thermal maturity (Chafeet et al., 2020). evaluated the source rocks potential and palynofacies of Early Cretaceous formations (Nahr Umr, Zubair, and Yamama) in Suba oilfield, southern Iraq and suggested that Yamama Formation has a good hydrocarbons potential in that area.

Previous studies by Iraqi and international oil companies operating in Iraq over the last few decades (e.g., (Beydoun et al., 1992), as well as some recent studies (e.g. (Pitman et al., 2004) (Al-Khafaji et al., 2021b)), indicate that the majority of the hydrocarbons accumulated in the Cretaceous and Tertiary reservoirs in the Middle and South of Iraq may have been generated by the Middle Jurassic Sargelu and Najmah formations. However, the huge quantities of hydrocarbons trapped in these reservoirs appear to be considerably higher than the Sargelu and Najmah formations can yield. Therefore, other mature source formations may have contributed to supplying oil to these reservoirs.

This study is recognized as one of the most significant organic geochemical investigations since it addressed one of the most important

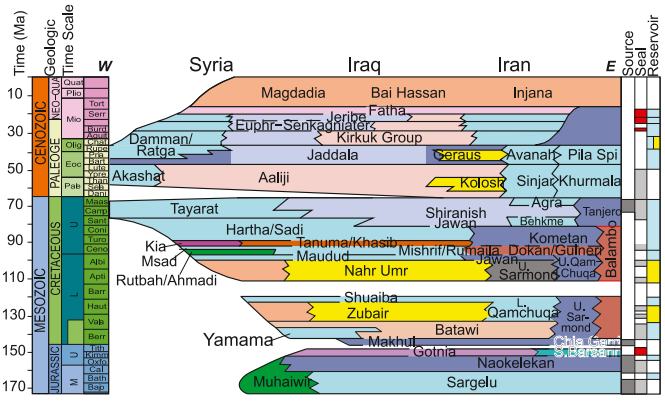

Fig. 2. Position of the Yamama Formation in the sequence stratigraphy of the latest.

formations in central and southern Iraq, the Yamama formation, which is regarded as one of the most probable source rocks for hydrocarbon generation and may have contributed to the generation and expulsion of hydrocarbons into neighboring reservoirs.

2. Geologic setting and stratigraphy

The Yamama Formation of southern Iraq represents the second lower part of a regressive cycle that extends from the Late Tithonian to the Upper Aptian and includes the Sulaiy Formation (sub-basinal); the Yamama Formation (inner and outer carbonate ramp); the Ratawi Formation (mixed clastic and carbonates system) and the Zubair Formation (fluvial and deltaic clastic system). The cause of this gradual change from the carbonate system of the Sulaiy Formation to the clastic system of the Zubair Formation was due to the establishment of a clastic front at the southwestern part of Iraq, (Aqrawi et al., 2010).

The clastic front resulted from the establishment of humid climatic conditions during Early Cretaceous, that generated a considerable amount of clastic material which started to move northward. Clastics increase from top Sulaiy upward, but formations are separated by time gaps and the process is thus not continuous up to the Zubair where clastic culminate. Shelf deformations, and not only climate but are also responsible for the erosion of uplifts, bringing detrital material.

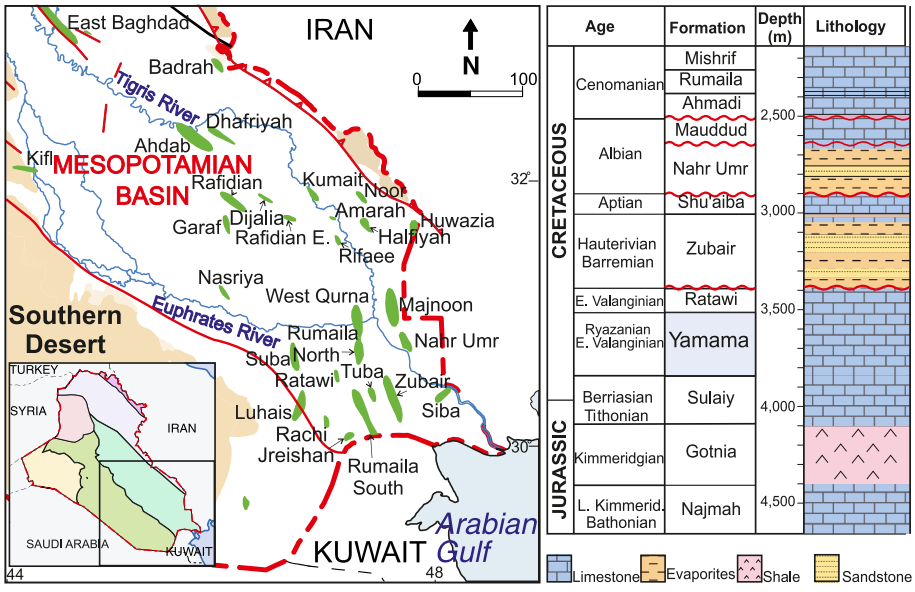

Fig. 1. Left. The major oil fields in central and southern Iraq are also shown on a map of the study area. Right. Stratigraphic section of the well Rumaila North (Ru-72), Southern Mesopotamian Basin, Iraq.

Fig. 3. Tectonic map of Iraq, Compiled and modified from (Buday and Jassim, 1984).

Moreover, this process is much more widespread regionally and were not restricted to southwestern Iraq.

Indications of such clastic invasion can be seen in the presence of frequent sand-bearing carbonates and some continental shaly materials within the Yamama Formation in southwestern Iraq particularly at its upper part. Such materials started to increase gradually in the overlying Ratawi Formation till it becomes the dominant lithology in the Zubair Formation pushing the carbonate system further northward. Thus, although the Yamama formation was deposited in a marine ramp, it has some continental components too (Sadooni, 1993). constructed a facies map of the Yamama sediments showing that the major carbonate facies of the formation were laid down in the inner ramp (Fig. 4 a). Furthermore, it was noticed that the lateral facies change is gradual. The study area is located in this context in a leeward position creating a relatively protected low energy depositional settings (Sadooni, 2010)

Also, at smaller scale, there is a clear differentiation in facies distribution of the formation on crests or on flanks of the structures, (Sadooni, 1993). This was attributed to the possible growth of the structures e.g., West Qurna and Rumaila, during the deposition of the Yamama Formation. Therefore, wells on the flanks have more mud-supported facies of argillaceous mudstone and wackestone compared to wells on the crests. Furthermore, it was noticed that the lateral facies change is gradual, and this was attributed to the leeward position of the study area creating a relatively protected low energy depositional settings, (Fig. 4b) (Sadooni, 2010).

3. Material and methods

The palynological and palynofacies work is based on forty core samples that were collected from ten of oil fields. These are Rumaila (wells R-9, R-167); West Qurna (well WQ-15); Suba (well SU-1), Luhais (well Lu-7); Halfiyah (well HF-2); Zubair (well ZB-45); Rachi (well R-131); Jerishan (well Jr-31, and Ratawi (well Rt-5). The dispersed organic matter was isolated by digestion with hydrochloric acid then with hydrofluoric acid. The macerate is completely cleansed and smeared with poly-vinyl alcoholic and Canada-balsam on a zero-glass cover. Visual estimations are used for the quantitative assessment of

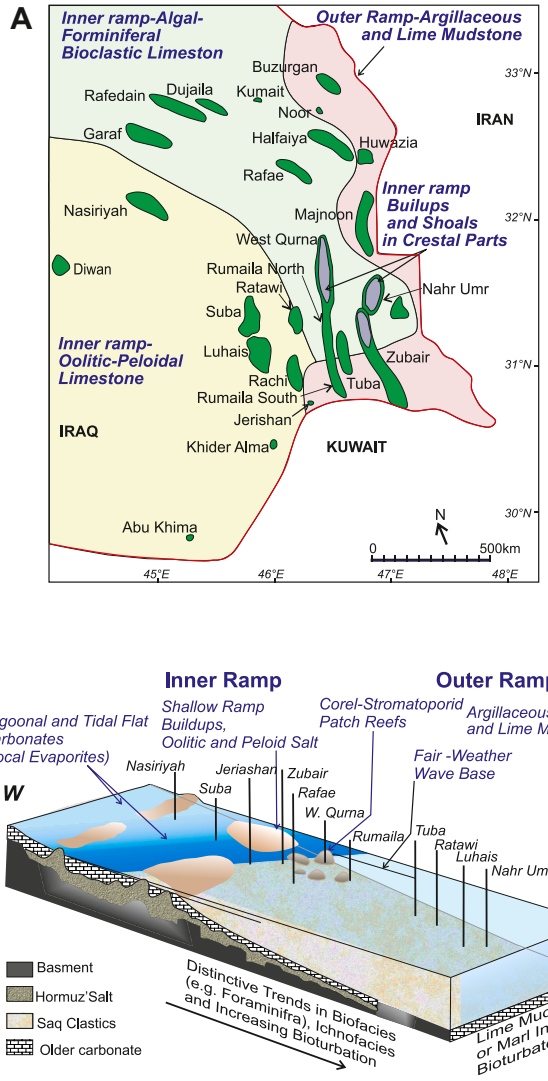

Fig. 4. A. depositional environment and Yamama Formation facies map of the (Sadooni, 1993), in southern Iraq. Fig. 4 B. A suggested 3-D model of the sedimentological setting of the Yamama Formation in the middle and southern Iraq, modified after (Sadooni, 1993).

the organic matter. The main advantages of kerogen microscopy are: It provides information on the relative abundance of the types of organic matter, the properties of the various components of the assembly of this organic matter, and through correlating this optical data with the obtained geochemical composition, we will get better results (Tyson, 1995)The organic matter extraction for the palynofacies study was carried out at the Department of Geology Laboratories, in the University of Baghdad.

Forty available subsurface source samples were selected from Di-1, Ga-1, Jr-1, Lu-12, NR-7, Mj-11, Ns-1, Rt-2, Rt-5, Rt-7, R/172, R167, Su-8, Tu-3, and WQ-15 wells. They were subjected to analysis using Rock-Eval pyrolysis to assess the source rock petroleum generation potential. Biomarker and carbon isotope analyses were performed on the thirty-one samples of the Formation collected from the Di-1, Kf-3, NR-9, Lu-13, Mj-12, NR-7, NS-1, Rt-5, Rifae-1, SU-8, WQ-15, WQ-60, Zb-44, and Zb-47 wells (Table 1; Fig. 5).

The TOC content (total organic carbon) was assessed by using LECO EC-12 carbon analysers. Most of the TOC and pyrolysis analyses were carried out at the laboratories of the *Oil Exploration Company* in Baghdad and the others are at *Geomark Research Ltd.*, Houston (Texas, USA). Other geochemical analyses include biomarker fingerprinting using

Table 1
The type of analyses and depth of the studied Yamama Formation samples.

No	Oilfield	Well	Depth (m)	Formation	Analyses
1	Diwan	Di-1	1225	Yamama	Biomarkers & Carbon Isotope
2	Diwan	Di-1	1213	Yamama	Biomarkers & Carbon Isotope
3	Diwan	Di-1	1235	Yamama	Biomarkers & Carbon Isotope
4	Diwan	Di-1	1198	Yamama	Biomarkers & Carbon Isotope
5	Diwan	Di-1	1201	Yamama	Biomarkers & Carbon Isotope
6	Diwan	Di-1	1204	Yamama	Biomarkers & Carbon Isotope
7	Diwan	Di-1	1207	Yamama	Biomarkers & Carbon Isotope
8	Diwan	Di-1	1210	Yamama	Biomarkers & Carbon Isotope
9	Diwan	Di-1	1222	Yamama	Biomarkers & Carbon Isotope
10	Diwan	Di-1	1300	Yamama	Biomarkers & Carbon Isotope
11	Diwan	Di-1	1225	Yamama	TOC & Pyrolysis
12	Garaf	Ga-1	3620	Yamama	TOC & Pyrolysis
13	Jershan	Jr-1	3909	Yamama	TOC & Pyrolysis
14	Jershan	Jr-1	3812	Yamama	TOC & Pyrolysis
15	Kifl	Kf-3	2630	Yamama	Biomarkers & Carbon Isotope
16	Luhais	Lu-12	3720	Yamama	TOC & Pyrolysis
17	Luhais	Lu-13	3730	Yamama	Biomarkers & Carbon Isotope
18	Majnoon	Mj-11	4030	Yamama	TOC & Pyrolysis
19	Majnoon	Mj-12	4030	Yamama	Biomarkers & Carbon Isotope
20	Nahr Umr	NR-7	3400	Yamama	Biomarkers & Carbon Isotope
21	Nahr Umr	NR-7	3349	Yamama	Biomarkers & Carbon Isotope
22	Nahr Umr	NR-7	3851	Yamama	Biomarkers & Carbon Isotope
23	Nahr Umr	NR-7	3320	Yamama	Biomarkers & Carbon Isotope
24	Nahr Umr	NR-9	3974	Yamama	Biomarkers & Carbon Isotope
25	Nahr Umr	NR-9	3759	Yamama	Biomarkers & Carbon Isotope
26	Nahr Umr	NR-9	3851	Yamama	Biomarkers & Carbon Isotope
27	Nahr Umr	NR-7	3393	Yamama	TOC & Pyrolysis
28	Nahr Umr	NR-7	3411	Yamama	TOC & Pyrolysis
29	Nahr Umr	NR-7	3431	Yamama	TOC & Pyrolysis
30	Nahr Umr	NR-7	3443	Yamama	TOC & Pyrolysis
31	Nahr Umr	NR-7	3536	Yamama	TOC & Pyrolysis
32	Nahr Umr	NR-7	3545	Yamama	TOC & Pyrolysis
33	Nahr Umr	NR-7	3556	Yamama	TOC & Pyrolysis
34	Nahr Umr	NR-7	3566	Yamama	TOC & Pyrolysis
35	Nahr Umr	NR-7	3665	Yamama	TOC & Pyrolysis
36	Nasiriyah	NS-1	3180	Yamama	Biomarkers & Carbon Isotope
37	Nasiriyah	Ns-1	3187.0	Yamama	TOC & Pyrolysis
38	Ratawi	Rt-5		Yamama	Biomarkers & Carbon Isotope
39	Ratawi	Rt-2	3916	Yamama	TOC & Pyrolysis
40	Ratawi	Rt-5	3708	Yamama	TOC & Pyrolysis
41	Ratawi	Rt-7	3803	Yamama	TOC & Pyrolysis
42	Ratawi	Rt-7	3744	Yamama	TOC & Pyrolysis
43	Rifae	Rifae-1	4200	Yamama	Biomarkers & Carbon Isotope
44	Rumaila N.	R/172	3700	Yamama	TOC & Pyrolysis
45	Rumaila N.	R/172	3700	Yamama	TOC & Pyrolysis
46	Rumaila N.	R167	3896	Yamama	TOC & Pyrolysis
47	Rumaila N.	R167	4094	Yamama	TOC & Pyrolysis
48	Rumaila N.	R167	4129	Yamama	TOC & Pyrolysis
49	Rumaila N.	R167	4210	Yamama	TOC & Pyrolysis
50	Rumaila N.	R167	3896	Yamama	TOC & Pyrolysis
51	Rumaila N.	R167	4094	Yamama	TOC & Pyrolysis
52	Rumaila N.	R167	4129	Yamama	TOC & Pyrolysis
53	Rumaila N.	R167	4210	Yamama	TOC & Pyrolysis
54	Rumaila N.	R-172	3550	Yamama	TOC & Pyrolysis
55	Rumaila N.	R-172	3605	Yamama	TOC & Pyrolysis
56	Rumaila N.	R-172	3655	Yamama	TOC & Pyrolysis
57	Rumaila N.	R-172	3751	Yamama	TOC & Pyrolysis
58	Suba	SU-8	3546	Yamama	Biomarkers & Carbon Isotope
59	Suba	Su-8	3585	Yamama	TOC & Pyrolysis
60	Suba	Su-8	3572	Yamama	TOC & Pyrolysis
61	Tuba	Tu-3	3775	Yamama	TOC & Pyrolysis
62	Tuba	Tu-3	3882	Yamama	TOC & Pyrolysis
63	Tuba	Tu-3	3885	Yamama	TOC & Pyrolysis
64	W. Qurna	WQ-15	3649	Yamama	Biomarkers & Carbon Isotope
65	W. Qurna	WQ-15	3684	Yamama	Biomarkers & Carbon Isotope
66	W. Qurna	WQ-60	3949	Yamama	Biomarkers & Carbon Isotope
67	W. Qurna	WQ-15	3649	Yamama	TOC & Pyrolysis
68	W. Qurna	WQ-15	3739	Yamama	TOC & Pyrolysis
69	Zubair	Zb-44	3994	Yamama	Biomarkers & Carbon Isotope
70	Zubair	Zb-47	3875	Yamama	Biomarkers & Carbon Isotope
71	Zubair	Zb-47	3958	Yamama	Biomarkers & Carbon Isotope

(GC) gas chromatography and (GC–MS) gas chromatography-mass spectroscopy. Stable carbon isotope analysis was carried out on 28 samples of source extracts from the same previous oil fields. These analyses were carried out at *Geomark Research Ltd*, Houston (Texas, USA) also.

4. Results and discussion

4.1. Palynofacies and paleoenvironment investigation

Palynofacies analysis is usually used to determine kerogen types, thermal maturity, and help in paleo-environment construction and understanding the depositional environments of organic matters within the sediments. Biochemical degradation, biomass productivity, and organic matter depositional processes are the main factors that influence the quality, and quantity of the kerogen of the organic matter which are accumulated in sediments (Tissot and Welte, 1984).

The study in the palynological assemblies is based on the occurrence of relative frequencies of amorphous organic material (AOM) up to 100% with a low amount of palynomorphs (AOM), phytoclast (macrophyte plant debris), and palynomorphs, as standardized by (Tyson, 1995). The value of total organic carbon (in weight %) and the increase in their thermal maturation determine their ability to generate hydrocarbons. To evaluate the type of kerogen and their hydrocarbon

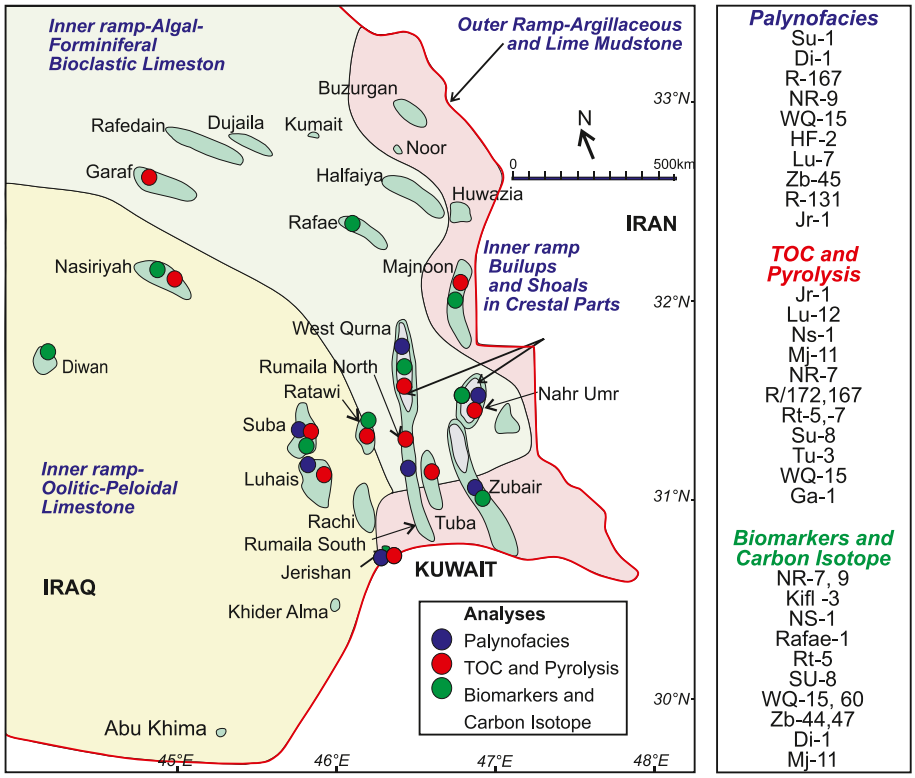

Fig. 5. A. Map representing the distribution of samples over the study area and the types of conducted analysis.

potential, the relative proportions of the palynomorph assemblages were plotted on the Tyson (APP) plot, (Fig. 6).

The depositional environment of the samples collected from the wells of Su-1, Di-1, Jr-1, and Zu-45 wells which fall in the field IX (Fig. 6, Left) represents a distal suboxic-anoxic environment, oil prone kerogen types II and I, and equivalent to carbonate which deposited in an inner ramp setting, (Sadooni, 1993); (Fig. 6, Right). Other samples (NR-9, R-167 and 131, WQ-15, Lu-7, and HF-2), that are in the field VIII suggest from distal suboxic–anoxic to dysoxic–anoxic environment with kerogen type II, which is equivalent to argillaceous and lime mudstone, (Sadooni, 1993) (Tyson, 1995). This may indicate variable depositional environments ranging from deep part of a ramp environment to a quiet, deep, and open marine basin as reflected by the presence of numerous dinoflagellate cysts and high percentage of AOM.

Although (Al-Siddiki, 1978) divided the Yamama Formation into three vertical stratigraphic units deposited within two major megasequences, these units are not correlatable over large areas. The wide variation in the facies and thickness of these units may be attributed to the previous topographic surface, tectonics, and different subsidence rates, this was confirmed by (Sadooni, 1993). The changes in lateral sedimentary depositional environments and are also accompanied by vertical changes within the same well. Fig. 7 shows the vertical differences within the same well, which is Rumaila-172, as at the depth of 3550 m the sample indicated a distal suboxic–anoxic to the

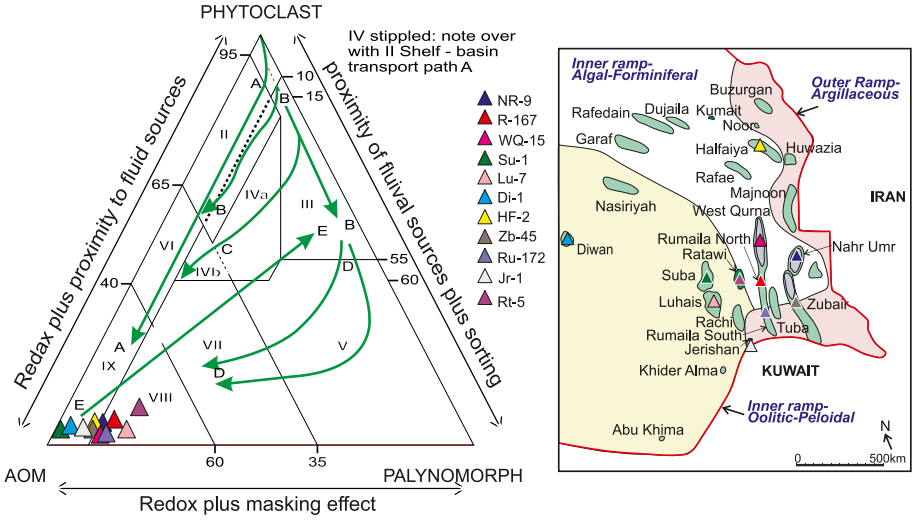

Fig. 6. Left; Ternary of the (AOM, phytoclast, and palynomorph) kerogen plot, of (Tyson, 1995) the Yamama source organic matters assemblages dominated by amorphous organic material (AOM) up to 100% with a low abundance of palynomorphs and the depositional redox conditions. Right; A map showing the locations of the studied samples.

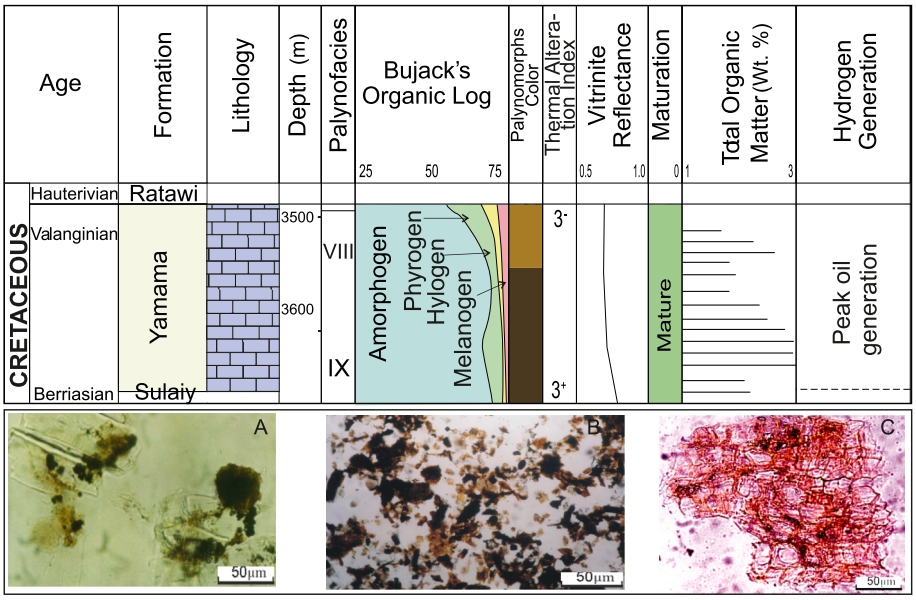

Fig. 7. Top; Organlog scheme of palynofacies and evaluation of the source potential for Lower Cretaceous Yamama Formation in Well Ru-172 of Rumaila South oil field, in Southern Mesopotamian Basin. Bottom; Palynofacies association retrieved from the Yamama Formation, of Rumaila South-72; A. Phytoclast, depth: 3520 m, B. Cuticle, depth: 3520 m C. A diverse AOM assemblage, depth: 3650 m.

dysoxic–anoxic environment (Type VIII), while at the depth of 3630 m it indicated a distal suboxic-anoxic environment (Type IX).

The palynofacies Type IX and VIII as shown in (Fig. 7) and in AAP ternary plot (Fig. 6) show that the Yamama source is at peak oil generation, and the organic matter (OM) was accumulated in anoxic basins, (Al-Ameri et al., 2009). The thermal Alteration Index for the Yamama samples range from (3- to 3+), which indicates a moderate to higher maturity at the main phase of petroleum generation, (Staplin, 1969); (Fig. 7A, B, C).

These results are for samples taken from random depths of the formation, according to available samples, and sometimes we notice vertical changes in the sedimentary facies in the same well, which reflect changes in the sedimentary facies over time, as shown in Fig. 6, where the sample taken from a depth of 3510 m from the Rumaila South oil field's Well Ru-172 reflected the Type VIII environment, while the sample taken from a depth of 3630 m reflected the Type IX environment.

4.2. 2. Evaluation of source rocks using Rock-Eval pyrolysis

4.2.2.1. Quantity and quality of organic matters. The other three, more easily defined geochemical factors that are used to assess the effective source using Rock-Eval pyrolysis are: (1) amount of organic matter, (2) type of organic matter, and (3) thermal maturity. It requires a short analysis time of about 20 min, needs a small amount of the sample, about 100 mg and it is less expensive. The quantity of organic carbon is determined by two useful measurements: the TOC, wt. % (total organic carbon) and the hydrocarbon index (HI) in the rock sample, (Peters, 1986). The nature of the hydrocarbons generated is greatly influenced by the type of sedimentary organic matters in the source rocks.

The TOC content of the Yamama Formation samples varies from 0.09 to 5.12 wt%, with an average of 0.86 wt%. Accordingly, the source rock's generative potential ranges from poor to excellent. The hydrocarbon potential is calculated in kg of hydrocarbons per ton of rock using two fractions: S1, free hydrocarbons, and S2, hydrocarbons liberated by cracking during pyrolysis. and S2 range from 0.02 to 11.31 and from 0.11 to 24.13, respectively. These parameters indicate that the OM quantity ranges from poor to excellent source rock hydrocarbon potential. The petroleum potential (S1+S2) vs TOC plotted in Fig. 8 shows that the Yamama source varies from poor to excellent.

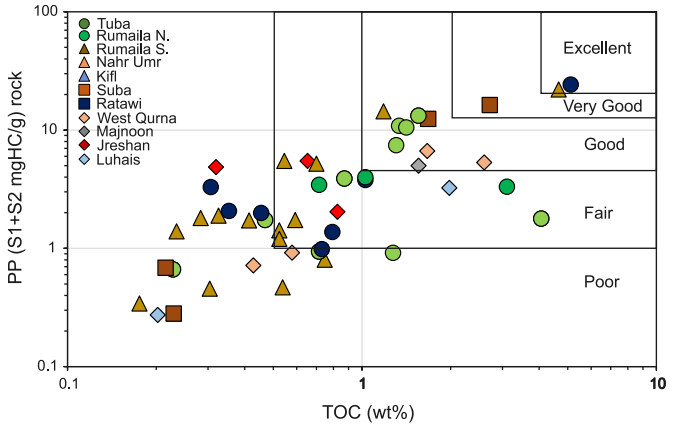

Fig. 8. Plot of the relationship between TOC% and S1+S2 for the Yamama Formation. In southern Iraq.

The HI (Hydrogen Index) values are ranging from 49 to 981 mg HC/g TOC, while the oxygen index (OI) is ranging from 0.27 to 77(mg CO_2/g TOC). Yamama samples show clearly, variable quantities of TOC, S2, and HI. These values reflect different depositional environments, which produced different types of organic matters, preserved in these rocks. Accordingly, most samples have kerogen types II, II/III and III, with some input of kerogen type I in few samples. Few samples from Nahr Umr and Suba oil fields have kerogen type I, many samples from West Qurna, Tuba and Jershan oil fields have kerogen type III, while all other samples have kerogen type III.

Pyrolysis S2 yield vs TOC, diagram (Fig. 9) can also be used to define quality and classify the kerogen types. The figure shows the prevalence of kerogen type II (oil prone) and III (gas prone). Few samples have kerogen type I, which is considered as a very oil prone, (Tissot and Welte, 1984).

These wide variations in the kerogen types are due to the different types of depositional setting and facies as discussed above. Some samples show a S1/TOC ratio that is higher than 0.2 with lower maturity suggesting migrated oils, (Peters, 1986).

Accordingly, the formation may have generated oils in Nahr Umr,

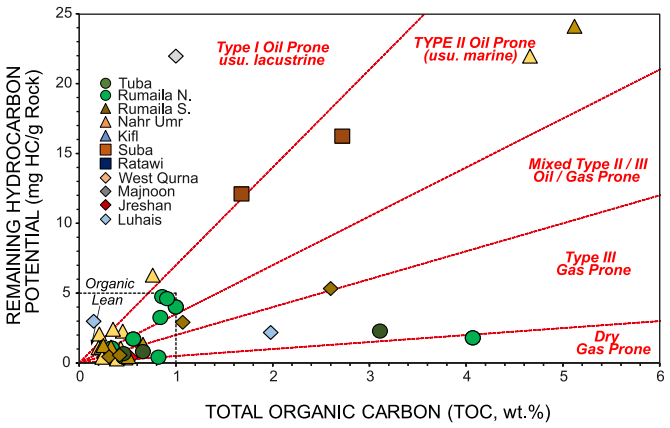

Fig. 9. Remaining hydrocarbon potential (S2) against total organic carbon (%) plot to determine the Kerogen quality for the Yamama source rocks in southern Iraq.

Rumaila North and South, and Ratawi oil fields, while in West Qurna, Majnoon, and Jerishan oil fields may have generated oil and gas, and considered as gas prone in Luhais, Tuba and Suba oil fields due to the variation in kerogen types.

4.2.2.2. Thermal maturity. The sedimentary organic matter buried in the source rock, due to the progressive subsidence of the sedimentary basin, will be exposed to an increase in temperature and pressure on it. The thermal maturity level can be estimated by using the Production Index (PI) [Production index PI = S1/(S1+S2)], and T*max*. (Peters, 1986).

Most of them have T*max* values that range from 430 °C to 451 °C. Some samples are considered mature sources at the beginning of the oil window and others are higher maturity at the top of the oil window and had reached the expulsion window. Other samples have T*max* value that are less than 430 °C, which are considered as immature source. The samples also have PI values in the range of 0.1–0.75. Most of them have values situated between 0.1 and 0.4 mg of HC/g TOC, indicating that they are within the oil window. Few samples have values over 0.4 which may indicate either the presence of commercial gas producing horizons or may be represents migrated hydrocarbons, (Tissot and Welte, 1984). Fig. 10 shows that most of the studied samples are mature, and these rocks generated and expelled oil and gas to the neighboring Cretaceous reservoirs, (Al-Khafaji et al., 2019a). In general, the thermal maturity stage begins in the oil fields west of the study area at a depth of 3431 m with a T*max* of 431 in the field of the Nahr Umr, while it increases as we

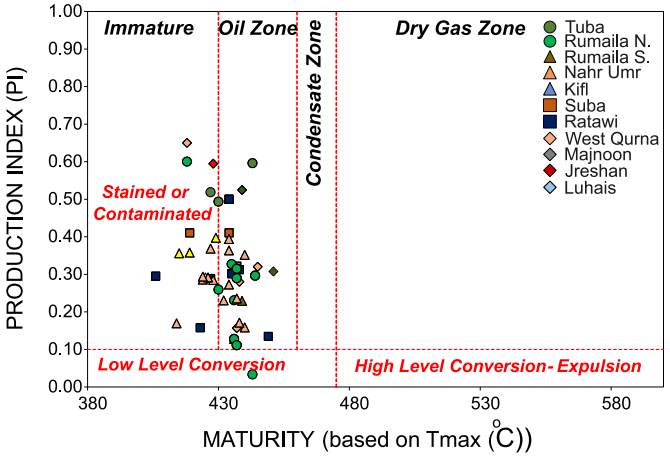

Fig. 10. Kerogen conversion and maturity plot (production index versus T*max*) for the Yamama source rocks in southern Iraq.

head east and south. The samples from West Qurna, Zubair, Tuba, Rumaila South, Luhais, and Nahr Umr oil fields are considered at higher maturity levels than others, taking into account the effect of burial depth, which is directly proportional to thermal maturity increase. This may due to the Late Eocene tectonic movements of the Arabian Plate, which caused the compression between the Arabian Plate and Eurasia and Zagros Inversion. This movement was caused because of the extension of the Red Sea and the Gulf of Aden which generated a substantial increase in pressures and temperature.

In Fig. 11, it is shown that the kerogen of Yamama source is distributed among types II, II/III, and III, and a few samples fall into the kerogen type I zone, and that most of the samples are located within the range of thermal maturity.

Because of the Yamama source contains kerogen of types II and III that resulted from current burial from 3270 m to 4210 m, as well they already at the peak of oil expulsion stage, so that the contribution of the Yamama source to the charge of oil and gas reserves to the Mesopotamian Basin is deemed worth considering, (Al-Khafaji et al., 2019b). Also, because pyrolysis maturity parameters (T*max* and PI) is affected by the type of organic matter (OM), (Peters, 1986), so that the (TAI), of (Tyson, 1995) as shown in (Fig. 7) is (3- to 3+), confirm the fact which is the Yamama source maturity levels were range from mature to higher maturity.

4.3. Biomarker and non-biomarker analyses

4.3.1. Depositional environment and types of organic matters

A suite of biomarker as well non-biomarkers ratios was applied to assess source redox condition and the source depositional environments, including pristane/phytane (Pr/Ph), Pr/nC_{17}, Ph/nC_{18}. Many source rocks that were derived from marine algae show abundant short-chain *n*

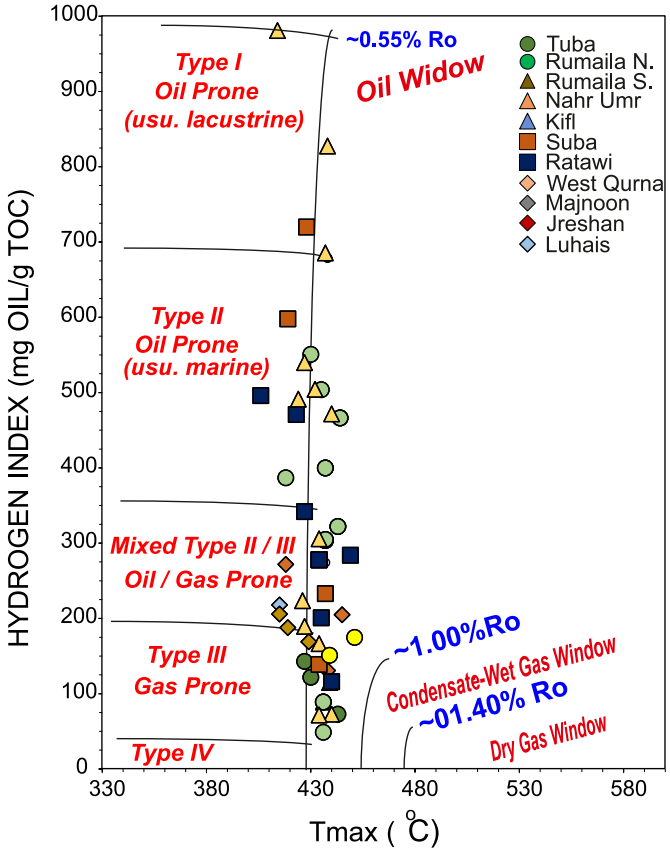

Fig. 11. The kerogen types and maturity levels of the Yamama source rocks in southern Iraq samples are plotted in this diagram.

- alkanes while those derived from higher plants exhibit a high prevalence of n-alkanes, (Peter et al., 2005). That because various factors influencing the quantity and quality of organic matter preserved in source rocks, such as organic matter input, sedimentation rate, and redox potential, so the biomarkers and stable carbon isotopes can allow a better assessment of organic matter input.

The distribution pattern of normal alkanes (Fig. 12) is within the range of n-C_{13} to n-C_{19} refers to marine organic matter with few contributions of land plant for Nasiriyah source sample, but in the Suba oilfield sample, there is no obvious land plants contribution, (Peter et al., 2005).

The chromatograms in (Fig. 12) show. bimodal biomarkers distribution of the Nasiriyah oilfield sample that refer to aquatic organic matter mixed with organic matter in addition to many land plants. Various common n-alkane and acyclic isoprenoids ratios are utilized to determine source input, depositional environments, and source rocks redox conditions, because of the easiness of its measurement using gas chromatography. The CPI (Carbon Preference Index) is common n-alkane ratios and influenced by maturity and source rock input. High CPI values suggest low maturity and terrigenous source input. While a value of CPI~1 indicates almost a predominance of the marine source input, (Peter et al., 2005). The carbon preference index (CPI), for the studied samples, is ranging from 0.94 to 1.06. Also, the short-chain n-alkanes relative abundance indicates that the variation in the organic matter input may reflect the variation in the depositional environment. The samples from Nahr Umr and Rifae oil field for example suggest aquatic organic matter input, and when it is matched with the facies map on (Fig. 4), they are located within the outer ramp but with a minor contribution of terrigenous component for Nasiriyah and Suba oil field samples, which are located within the inner ramp. Pristane and phytane are the most important acyclic isoprenoid hydrocarbons present in the source rocks and oil. The acyclic isoprenoid (Pr/Ph) ratio is believed to be the most redox condition indicator used (Didyk et al., 1978) method. The pristane/phytane ratio of the studied samples are ranging from 0.16 to 1 which confirms the marine input and indicates an anoxic to suboxic carbonate environment. The Pr/nC$_{17}$ versus ph/nC$_{18}$ plot also supports the reducing condition and indicates a thermally mature marine algal organic matter type IIs and a mixed marine and terrigenous input (type II/ III). In Fig. 13, the samples collected from the Nahr Umr, Nasiriyah, and Suba oil fields are located within the Terrigenous Type III zone, and except one sample from Nahr Umr oilfield appears within the Marine Algal Type II zone, while all other samples are located in the Type II/III mixed zone, which indicates that the Yamama source in Nahr Umr, Nasiriyah, and Suba oil fields area contain more terrigenous input, which reflect a considerable variation in the depositional environment. This fully corresponds to the results obtained from the pyrolysis analyzes, and the relationship of hydrogen

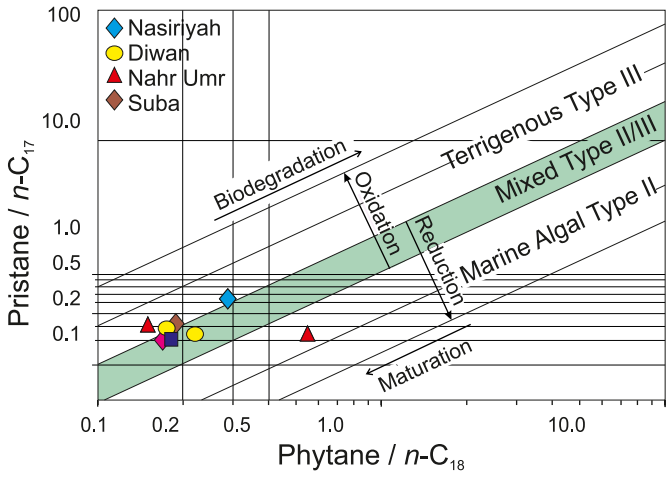

Fig. 13. The Pr/n-C_{17} versus Ph/n-C_{18} cross-plot for the identifying deposition environments, source input, and thermal maturity of the Yamama source samples from studied oil fields, southern Iraq.

index with the T*max*, see (Fig. 11).

The carbon stable isotope compositions of the kerogen can be used with biomarker ratios to identify the marine and non-marine depositional environment, (Sofer, 1984). The carbon isotope analysis values of $\delta^{13}C$ (‰) saturated and $\delta^{13}C$ (‰) aromatic hydrocarbons for the Yamama source extracts are ranging from −28.24 to −26.59, and −27.97 to −25.88 respectively. The stable carbon isotope ratios cross-plot for saturated and aromatic hydrocarbons, (Fig. 14), shows considerable differences between the samples. Most samples fall below the boundary line of (Sofer, 1984).

This indicates a marine organic matters input. It shows also that this trend is consistent with other Lower Cretaceous extracts, (Al-Khafaji et al., 2019a). The samples from Nasiriyah, Zubair, and Nahr Umr Oil fields seem to be close to the Sofer Line (Fig. 14), which may indicate some terrestrial organic matter. This confirmed the variable depositional environments, ranging from a deep shelf environment to a quiet open marine basin. The more negative the canonical variable value is, the more marine organic matters input, and vice versa. The values of the (CV) for the samples are ranging from −0.45 to −2.89 suggesting varied source depositional environments ranging from marine to more confined environments, (Sofer, 1984).

A suite of biomarker ratios (Terpene and Sterane) is used in this study to provide the geologic interpretations to source assessment, and depositional environments, (Fig. 15).

The mass fragmentograms for tricyclic terpane and hopanes (m/z 191), (Fig. 15, left), and steranes (m/z 217), (Fig. 15, right), of some

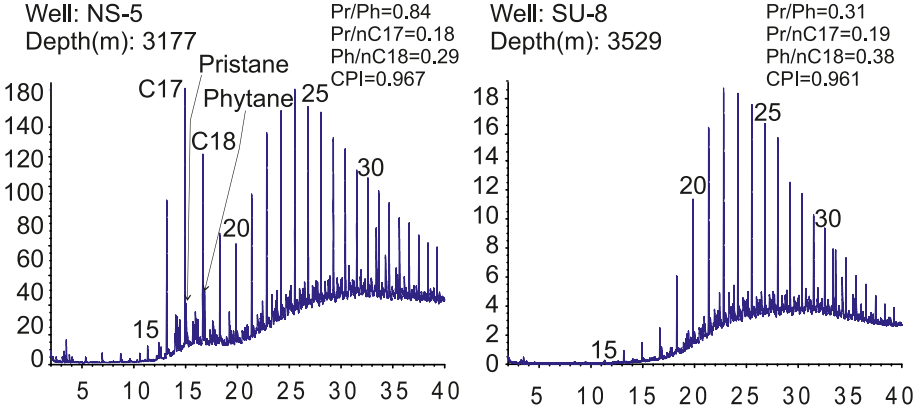

Fig. 12. Yamama source extract Gas chromatograms of the saturated fraction obtained by gas chromatography (GC-FID) for two selected Yamama samples (Ns-1 well chromatograms, (top), and SU-8 well, (bottom), southern Iraq.

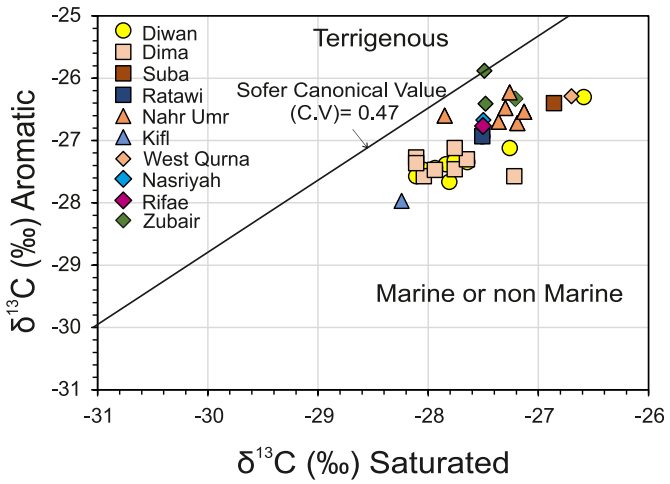

Fig. 14. Cross-plot of Stable Carbon Isotope Composition δper mil PDB (δ^{13}Caromatic versus δ^{13}Csaturated) for the analyzed samples.

selected samples (NS-5 and SU-8) are representative. The dominance of the C_{23}, and the low amounts of C_{19} and C_{20} tricyclic terpanes, refer to algal precursors, and minor terrigenous component input in some samples, (Peter et al., 2005). The C_{19}/C_{23} tricyclic terpanes ratio varies from (0.01–0.23) and indicates different depositional environments. The varying amounts of C_{19}/C_{23} tricyclic terpanes ratio also suggest different types of organic matter input. Samples from Dima, Diwan, and West Qurna oil field have higher ratio of C_{19}/C_{23} than the other samples indicating marine organic matter without a clear contribution from a terrestrial input. On the other hand, the samples which were taken from the Nasiriyah, Ratawi, and Zubair oil fields contain marine input with some contribution from land plants, (Figs. 4 and 19).

Various tricyclic terpanes and hopanes ratios; C_{22}/C_{21}, C_{24}/C_{23} (Fig. 16A), and C_{26}/C_{25} tricyclic terpanes, C_{31}/C_{30} hopane (Fig. 16B) used to distinguish the marine carbonate from the other source rock depositional environments. A high C_{22}/C_{21} ratio with an average of 1.18 and low C_{24}/C_{23} tricyclic terpane ratios with an average of 0.3 discriminate a carbonate-rich source. The C_{26}/C_{25} tricyclic terpane (<1.0) and C_{31} 22 R-hopane/C_{30} αβ ratio (>0.25) for the studied samples vary from 0.55 to 1.15, and 0.26 to 0.52 respectively, indicate anoxic marine carbonate deposition.

The C_{29}/C_{30} ratio defines the source rock facies. The 30-Norhopane/hopane or C_{29}/C_{30} hopane greater than 1.0 (Fig. 16C) indicates an anoxic carbonate and marl source rocks, (Peter et al., 2005). There is a wide variation in the C_{29}/C_{30} hopanes, in the studied samples ranging from 0.44 to 1.88 indicating varied depositional environments. The C_{35} homohopane index is considered as a common toxicity degree biomarker parameter in marine sediments, (Peter et al., 2005). High C_{35} homohopanes/C_{34} hopane (>0.8) and high C_{29}/C_{30} hopanes ratio (>0.6) indicates anoxic carbonate source rock and consist of high hydrogen index (HI) in source because the sedimentary organic matters would be more preserved in the anoxic basin. The wide variation among the $C_{35}S/C_{34}S$ ratio (0.43, to 1.31), and the C_{29}/H ratio ranges from 0.44 to 1.88 (Fig. 16 D) support also a variety of source environments and lithologies ranging from marine carbonates and marl to confined marine environments.

The Gammacerane (GA) is typical of saline to hypersaline depositional environments. Low gammacerane index ($Ga/C_{31}R$) and high pristane/phytane in source rocks indicate low salinity in the depositional basin (Fig. 17A). The C_{24} tetracyclic terpane ratio or Tet/C_{26} tricyclic is a carbonate depositional environment indicator. The C_{26}/Ts and Tet/C_{23} ratios are common source biomarker parameters. The C_{26}/Ts ratio with an average of 0.25 and the higher values for the Tet/C_{23} ratio, (Fig. 17B), which ranges from 0.66 to 1.52 also suggest marine carbonate source rocks deposited in a shallow intrashelf basin. The variation in the values of these ratios, reflect a variety of the source rocks depositional environments and lithologies ranging from anoxic

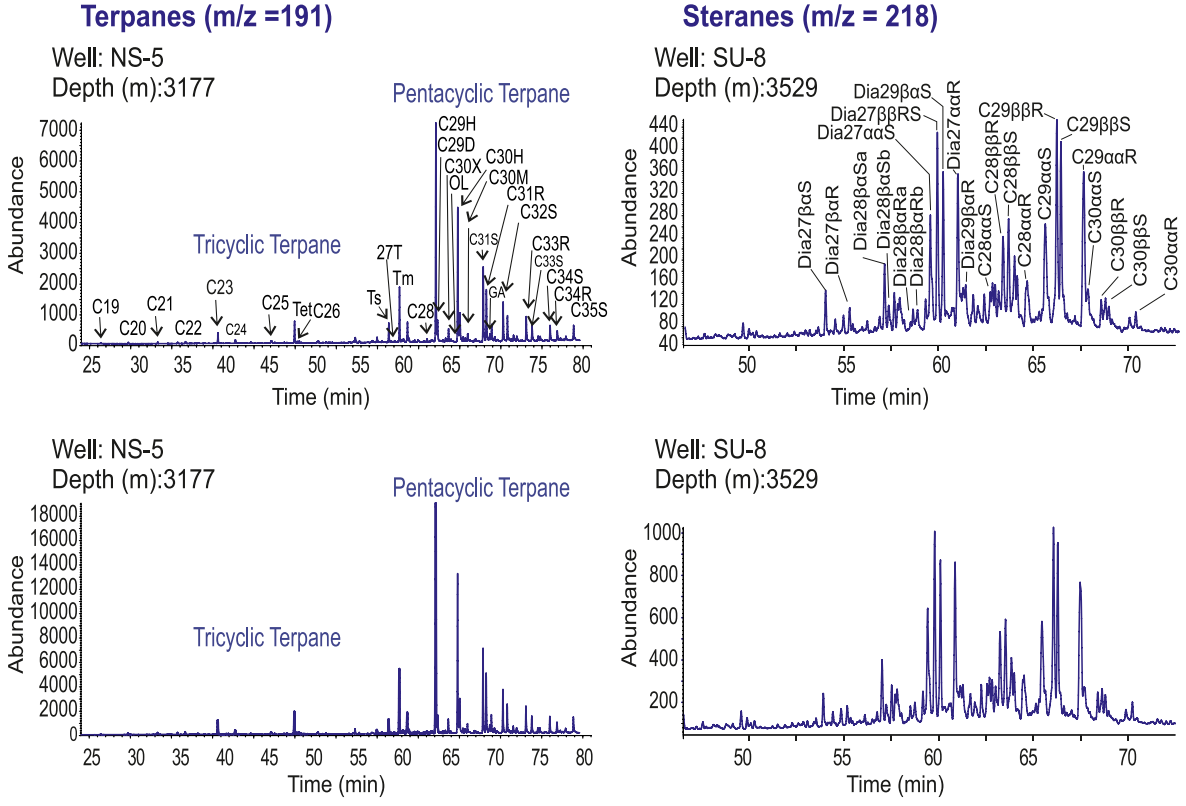

Fig. 15. Example of Yamama source extract chromatograms obtained by (GC-Ms) from Ns-5 and Su-8 wells.

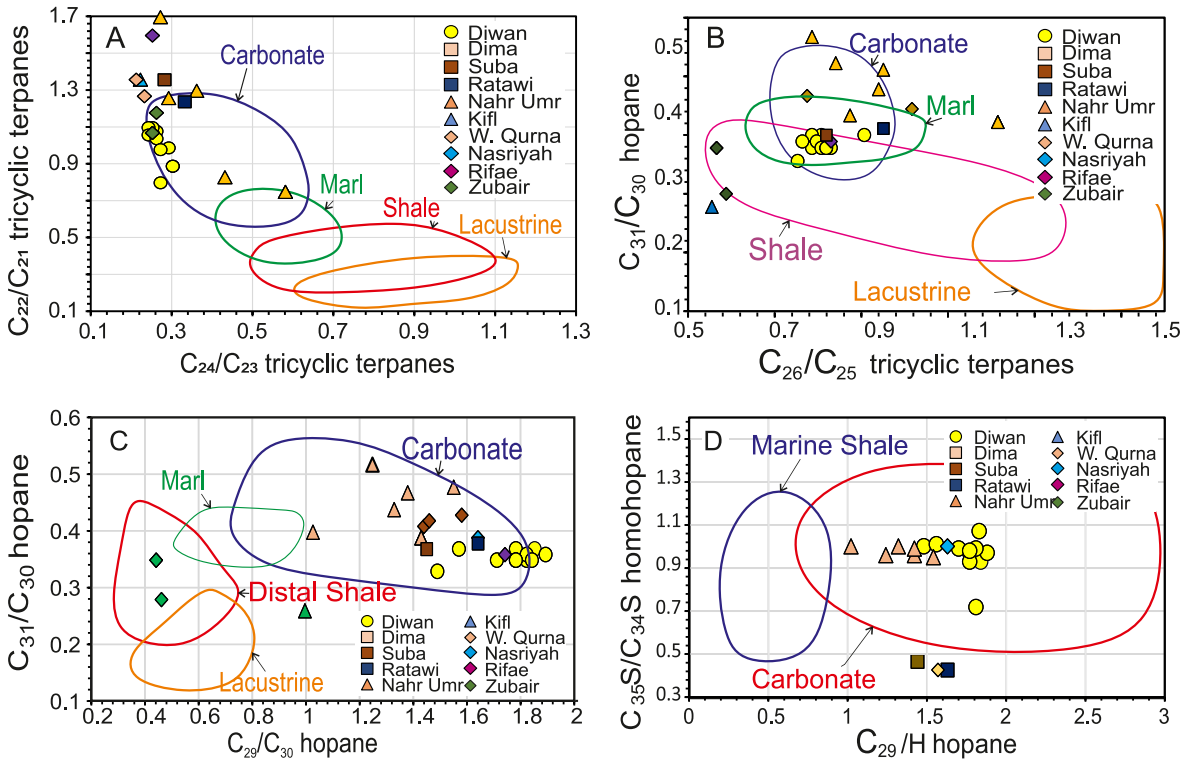

Fig. 16. Many tricyclic terpanes and hopane biomarker ratios used to define the depositional environments and source rock facies, support a variety of source environments and lithologies of Yamama source rocks, southern Iraq.

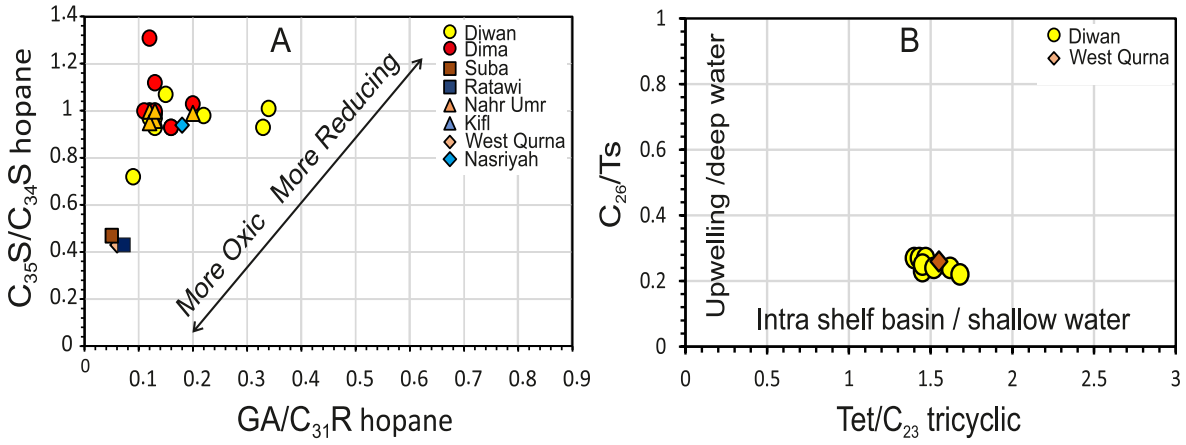

Fig. 17. (A) $C_{35}S/C_{34}S$ hopane versus $GA/C_{31}R$ hopane plot shows a variety of depositional setting. (B) The C_{26}/Ts versus Tet/C_{23} plot shows variety in depositional environments.

carbonate under open-water conditions to suboxic inland peat swamps.

4.3.2. Thermal maturity from saturated biomarkers

Many saturated biomarker parameters are employed as indicators of thermal maturity. The C_{27} Ts/Tm, C_{29} 20 S/R (8α-30-norneohopane), and TAS3(CR) ratios are used roughly to estimate the level of thermal maturity, because these parameters are usually affected by source facies and maturity, (Peter et al., 2005). The TAS3 ratio is considered as the most reliable indicator of thermal maturity because it is not dependent on the source (Zumberge et al., 2005) while the C_{27} Ts/Tm terpane is mostly dependent on source facies. The C_{29} ααα 20S/20 R sterane ratio is considered a sensitive biomarker for maturity because it increases with thermal maturity and but depends less on lithology.

The C_{27} Ts/Tm, C_{29} 20 S/R, (Fig. 18A), and TAS3(CR) ratios (Fig. 18B) for the studied samples are ranging from (0.06–0.8), (0.47–2.32), and (0.09–0.47) respectively. Samples collected from West Qurna, Zubair, and Nahr Umr oil fields are almost higher in maturity than those of Diwan, Ratawi, Kifl, and Suba oil fields. This variation in the values, clearly indicates a difference in the level of thermal maturity of the Yamama source samples and confirms that the samples were in early mature to peak stage and oil generation, (Zumberge et al., 2005); Peter et al., 2005). These conclusions are compatible with the Rock-Eval Tmax values of the samples, which range from 430 °C to 451 C°, indicating peak stage of oil generation and expulsion.

4.4. Petroleum generation modeling

4.4.1. Previous work

Basin and petroleum generation modeling is an important tool for integrating various geological and geochemical data. One dimension (1-

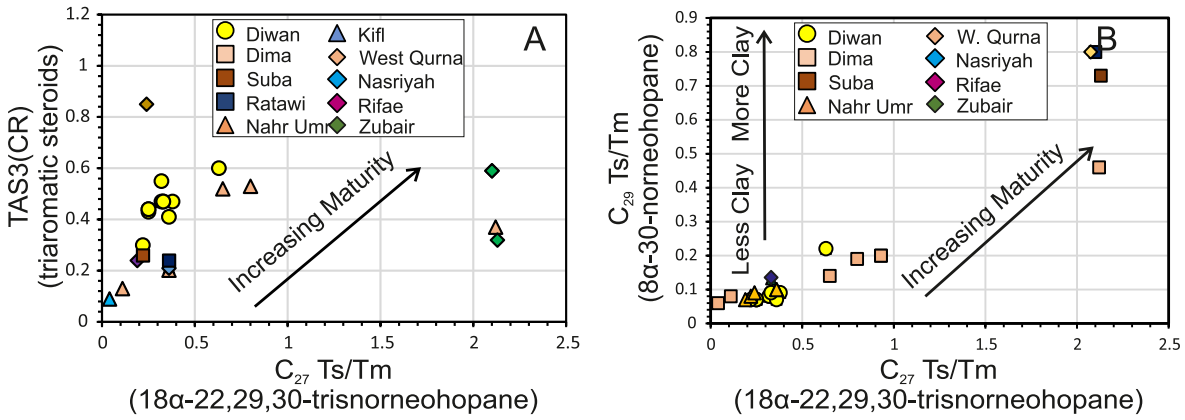

Fig. 18. The plots of (A) the C_{27} Ts/Tm terpane versus trichromatic sterane ratio (TAS3), and (B) with C_{29} 20 S/R.

D) models have been constructed using the *PetroMod* software to build the models of the thermal maturity, burial history, hydrocarbons generation history, which can optimize source rock assessments, petroleum generation history, expulsion, accumulation, and evolution of sedimentary basins of the studied source rocks, as well its possible capacity to contribute to the oil expulsion to neigboring reservoirs, (Waples, 1988).

(Pitman et al., 2004) combined the thermal history and the fluid-flow modeling of the Mesopotamian Basin, Iraq, and suggested that the peak oil generation of most of the Jurassic source rocks in the Basin occurred when the kerogen-oil transformation ratio (TR) exceeded ≥0.50 and reaching values ≥ 0.95, so oil generation and expulsion was completed and then it migrated during and after the late Miocene to the reservoirs (Abeed et al., 2013). built a 3-D basin model for the southern Mesopotamian Basin, based on limited organic geochemical and seismic data. They suggested that the Yamama source were within the oil window. They reported that the Yamama OM maturation began during the Cretaceous, but did not contribute to generating oil and expelling it to nearby reservoirs, (Al-Ameri et al., 2009); (Al-Ameri et al., 2011) discussed the hydrocarbon-charge modeling of the Cretaceous and Jurassic source rocks. They concluded that the Middle Jurassic Sargelu source had contributed in charging the Cretaceous reservoirs with petroleum (Aqrawi and Badics, 2015). investigated the burial, maturity evolution and petroleum generation of the Middle Jurassic–Lower Cretaceous source of the Mesopotamian Basin, and suggested that the Sargelu and Najmah formations are the best potential source rocks (Al-Khafaji et al., 2021). studied oil properties and basin modeling of source rocks in southern Iraq. They concluded that some of the oils were generated from the Late Jurassic and Early Cretaceous formations. While other oils are derived from the formations of the Middle Jurassic period. The previous studies mantioned above have shown that the sedimentary organic matter in the Yamama rock generated oil, but it hasn't been proven that the oil migrated and was trapped in the Cretaceous reservoir. Using biomarker technology and carbon isotopes, (Al-Ameri et al., 2009); (Al-Khafaji, 2015); (Al-Khafaji et al., 2018) concluded that the organic matter within the Sulaiy and Yamama rocks have generated oil and that the oil accumulated in the Mishrif Reservoir which constituted 30% of the total oil trapped of south Iraq is derived from these organic matter (Al-Khafaji et al., 2019a; Al-Khafaji et al., 2019b) study also, confirmed that the oil accumulated in the Yamama Reservoir in some wells of that study is originated from the Yamama Formation itself.

4.4.2. *Present work*

Local geothermal gradients, bottom-hole temperatures (BHT), thermal conductivity, source geochemical analysis, and other data as listed in Table 2, which were obtained from five wells in five oil fields, Majnoon (Well-8), Zubair (Well-47), West Qurna (Well-15), Nahr Umr (Well-9), and Nasiriyah (Well-1) that cover the study area, were used to construct a present heat flow, which, together with the paleo-heat flow in studied wells, would be needed to reconstruct oil well model calibration, as well as burial, thermal history, and the timing and extent of oil generation models (Fig. 19A and B).

Heat flow is influenced by tectonic activity, where the average of geothermal gradients becomes low with rapidly deposited sediment and increases with high sedimentation (Burrus and Audebert, 1990). The calculated geothermal gradients' best-fit heat flows (45–48 mW/m2) applied in the study area appear to be lower than usual regional heat flows of 60–65 mW/m2, possibly due to the high rate of sedimentation throughout the Late Miocene and Pliocene, (Fig. 19 D) (Pitman et al., 2004). Based on the thermal simulation results, the calculated geothermal for the studied wells varied locally from 17 to 20 °C/km, which is consistent with the published temperature gradient for the area. (Ibrahim, 1984).

At the Nasiriyah oil field (Well-1), the best fit between the borehole temperature and the current temperature was established at 28 °C (Fig. 20A and B). The maximum temperature for source rock is about 128.95 °C at a depth of 3600 m. The burial history model of the Ns-1 well (Fig. 20 C) shows two tectonic uplifts, one during the Late Cretaceous as a result of the Arabian Plate collision with Eurasia's continental blocks, and one during the Late Miocene-Early Pliocene as a result of the Zagros Orogeny activity. The thermal history model and curve display show that the Yamama source interval onset of the oil window (%Ro from 0.55 to 0.7) occurred around 86 Ma in the Early-Upper Cretaceous, reached the peak oil window (%Ro from 0.7 up to 1.0) at around 66 Ma in the Early Paleocene, and the late oil window of the organic compounds of Yamama source intervals occurs around 50 Ma in the Early Eocene, corresponding with (% Ro around 1.0 and greater). The high maturities ranging from 0.8% to 1.1% Ro were obtained locally in intrashelf basins having active source rock from the Late Oligocene to the onset of the Late Miocene. This may have been due to the rapid sediment accumulation that occurred due to the opening of the Neo-Tethys Ocean during the Zagros Orogeny, from the late Miocene to the Pliocene, resulting in a significant increase in source rock maturity along the foredeep. The oil transformation (TR) and thermal maturity curves (Fig. 20-D) indicate that oil generation started (TR > 10) in the Late Cretaceous (103 Ma) at a Vitrinite Reflectance (%Ro) of about 0.5 (temperatures of about 80 °C) and reached end generation (TR > 0.95) in the Late Eocene at 0.8 %Ro. Where (TR) denotes the transformation ratio of total petroleum generated to total petroleum generated by the kerogen.

The Yamama source in WQ-15, MJ-8, NR-9, and ZB-47 began to generate and expel oil in the Late Cretaceous (approximately 62, 75, 74, and 80 Ma) with a TR ratio of 10–50%, and reached its peak oil generation (TR 50–95%) from the Early to Late Paleogene (approximately 37, 24, 50, and 66 Ma). The Late Paleogene to Neogene (around 5, 7, 12, and 25 Ma) signaled the end of the time of oil generation (TR > 95% of

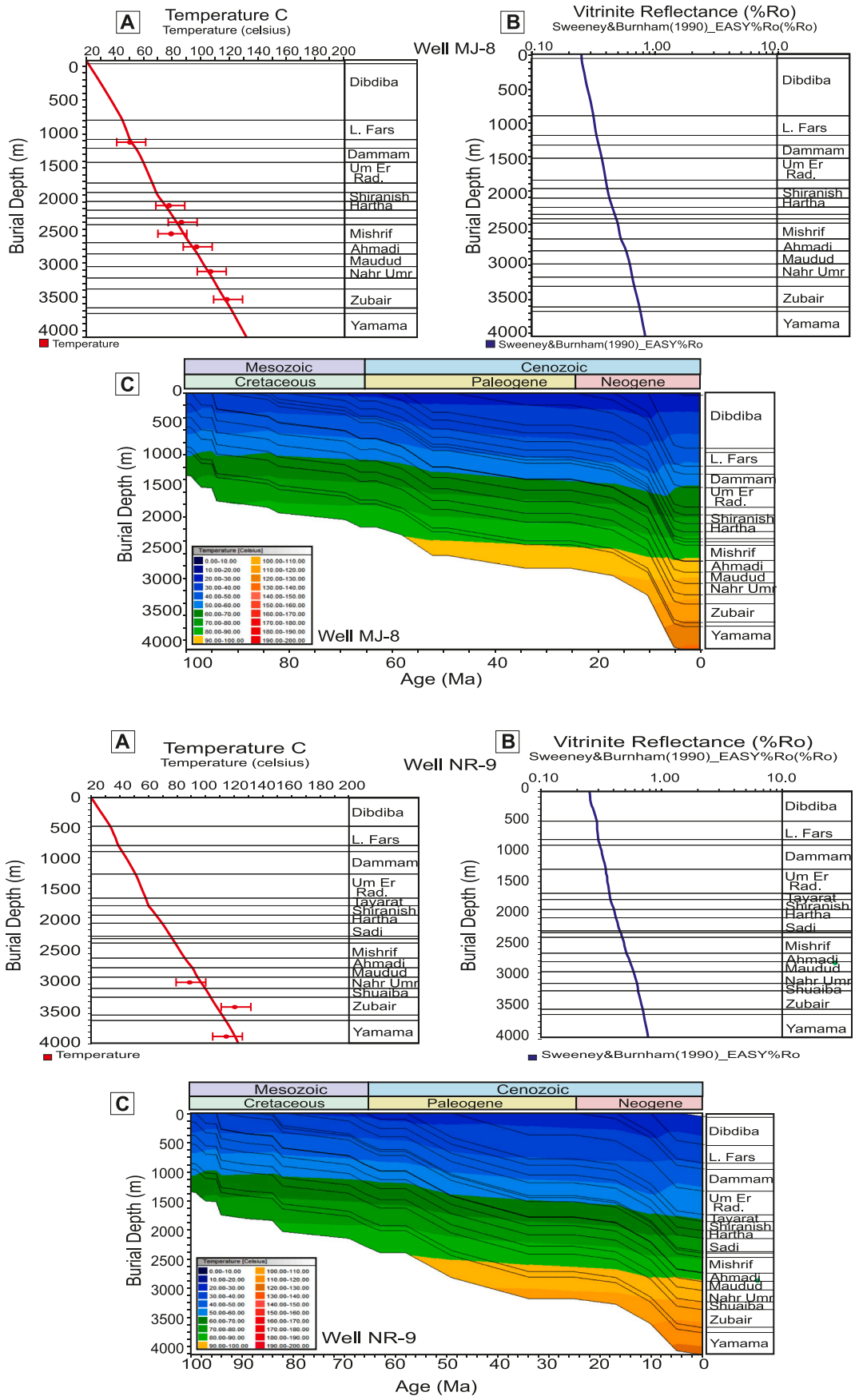

Fig. 19. A: Temperature is used to predict the best fit of the current heat flow in the MJ-8 we. B: A vitrinite reflectance calibration model for the MJ-8 and NR-9 wells. C: The burial temperature history model for the MJ-8 and NH-9 wells.

Table 2
The NS-1 well data set includes chronostratigraphic units, formation tops, and the ages of depositional and erosional events in the area of study.

Layer	Top (m)	Base (m)	Thick (m)	Eroded (m)	Depo from(Ma)	Depo to (Ma)	Eroded from(Ma)	Eroded to (Ma)	Lithology	PSE	TOC %	HI mgHC/gT
Dibdibba	348		348		10.8	8.9			SANDcongl	Overburden Rock		
lower Fars	519		171		15.3	10.8			LIME&EVAP	Seal Rock		
Ghar	894.8		93.5		22.1	17			SANDcongl	Overburden Rock		
Dammam	988.3		115.7		36	33.7	33.7	22.1	LIMEdolom	Overburden Rock		
Rus	1104		8		48.8	47.8			LIME&EVAP	Seal Rock		
Umm ErRathuma	1112		595		62.9	51.1			LIME&EVAP	Seal Rock		
Tayarat	1707		130		69.6	66.9	66.9	62.9	LIME&EVAP	Reservoir Rock		
Shiranish	1837		119.5		72.5	69.6			LIMEmarly	Source Rock		
Hartha	1956.5		179.5		78.7	72.5			LIMEmarly	Reservoir Rock		
Sadi	2136		141.7		84.9	80.3	80.3	78.7	LIMESTONE	Reservoir Rock		
Tanuma	2277.7		47.3		85.9	84.9			SHALE	Reservoir Rock		
Khasib	2325		63.4		91.8	85.9			LIMEmarly	Reservoir Rock		
Mishrif	2388.4		172.6		94	92.3	92.3	91.8	LIMESTONE	Reservoir Rock		
Rumaila	2561		71.8		95.7	94			LIMEshaly	Overburden Rock		
Ahmadi	2632.8		14.5		97.2	95.7			SHALE	Overburden Rock		
Mauddud	2647.3		278.9		101.4	99.4	99.4	97.2	LIMESTONE	Reservoir Rock		
Nahr Umr	2926.2		208.2		109.6	101.4			SANDshaly	Reservoir Rock		
Shuaiba	3134.4		94.1		120.7	113.2	113.2	109.6	LIMESTONE	Reservoir Rock		
Up. Shale mbr	3228.5		330.8		121	120.7			SHALEsand	Source Rock	0.585	117.3028
up. Sandstone mbr	3338		92		123	121			SANDshaly	Reservoir Rock		
Mid. Shale mbr	3430		77		124	123			SHALEsand	Source Rock		
L. Sandstone mbr	3507		33		125.5	124			SANDshaly	Reservoir Rock	0.678	74.94039
L. Shale mbr	3540		19.3		127.4	125.5			SHALEsand	Source Rock		
Ratawi	3559.3		130.7		135.9	131	131	127.4	LIMESTONE	Reservoir Rock		
Yamama	3690		205		143.1	135.9			LIMEdolom	Reservoir Rock	1.7	272
Sulaiy	3895		240		148	143.1			LIMEshaly	Source Rock		
Gotnia	4135		??		154	148			EVAPORITE	Seal Rock		
Geothermal Gradient = 0.018 c./m.			surface temp. = 20 °C			BHT = 103 °C at 3690 m.			Note: all tops are from R.T.K.B. = 12.65 m.			

total), and it has continued to the present day (Fig. 21A and B). The TR was 100 percent generation at the time of the study for all wells except NR-9, which was 98 percent. According to burial history, thermal maturity, and oil generation timing models, for the studied wells, the Yamama Formation was buried at a depth ranging from 3900 to 4200 m, with a maximum temperature of 118 °C (Figs. 19C and 20C), and entered within a main oil generation window and reached a very high conversion rate of TR = 100 percent, which resulted in the expulsion of large quantities of crude oil from the source-interval layers and is still occurring in some wells presently (Fig. 21A and B). There is currently a regular increase in thermal maturity from west to east across the study area, demonstrating that Yamama source rock maturation is mostly regulated by burial.

The burial-thermal models revealed that the Yamama formation entered the oil generation window and completed oil generation earlier in the oil fields west of the study area, such as the Nasiriyah, and Zubair oil fields, at a burial depth ranging between 3177 and 3421 m, and 3658–4043 m, respectively, compared to fields located to the east, such as the Nahr Umr oilfield, which was at a depth ranging between 3741 and 4113 m, notwithstanding the typical increase in thermal maturity from west to east of the study area.

5. Implications

The Yamama Formation depositional system covered a wide leeward carbonate ramp that extended from west to east in the central and southern parts of the Mesopotamian Basin. The ramp was divided into an inner ramp, where the Yamama Formation is formed mostly of grain-supported textures such as oolitic and peloidal packstone and grainstone with local coral-stromatoporoidal facies, and an outer ramp, where the Yamama is formed of locally bioturbated, mud-supported facies with some marls and marly limestone, (Fig. 4 A and B). Some parts of the ramp were subjected to a terrestrial influx due to climatic and tectonic conditions from time to time. The vertical succession of the whole sections indicates a tendency toward increasing the clastic input upward.

The wide variation in the sedimentary facies of the Yamama formation may be due to many factors that have influenced the development of complex facies patterns in the Yamama Formation, both vertically and horizontally (Sadooni, 1993). mentioned the following factors: The Yamama basin is covered by two different tectonic units. Ancient changes in sea level may have led to changes in the lithology and sedimentary depositional environments of the formation, as well as the variation in symmetry and the slope of the structures. Sometimes, correlations between two adjacent oil wells can be difficult at times. In limited cases, the conclusion may not be obvious when comparing the kerogen type and the location maps of the oilfields from Fig. 22. The type may seem random compared to the location and depositional setting at this scale. Because the depositional environments and clastic inputs vary with time along the stratigraphic column, the result may depend on the sample location in the stratigraphy and on the sedimentological characters at this time. The sample petrography is not fully available for the authors to assess precisely this relationship.

The geochemical analysis results for this study reflected the complex depositional situation and the obvious changes vertically and

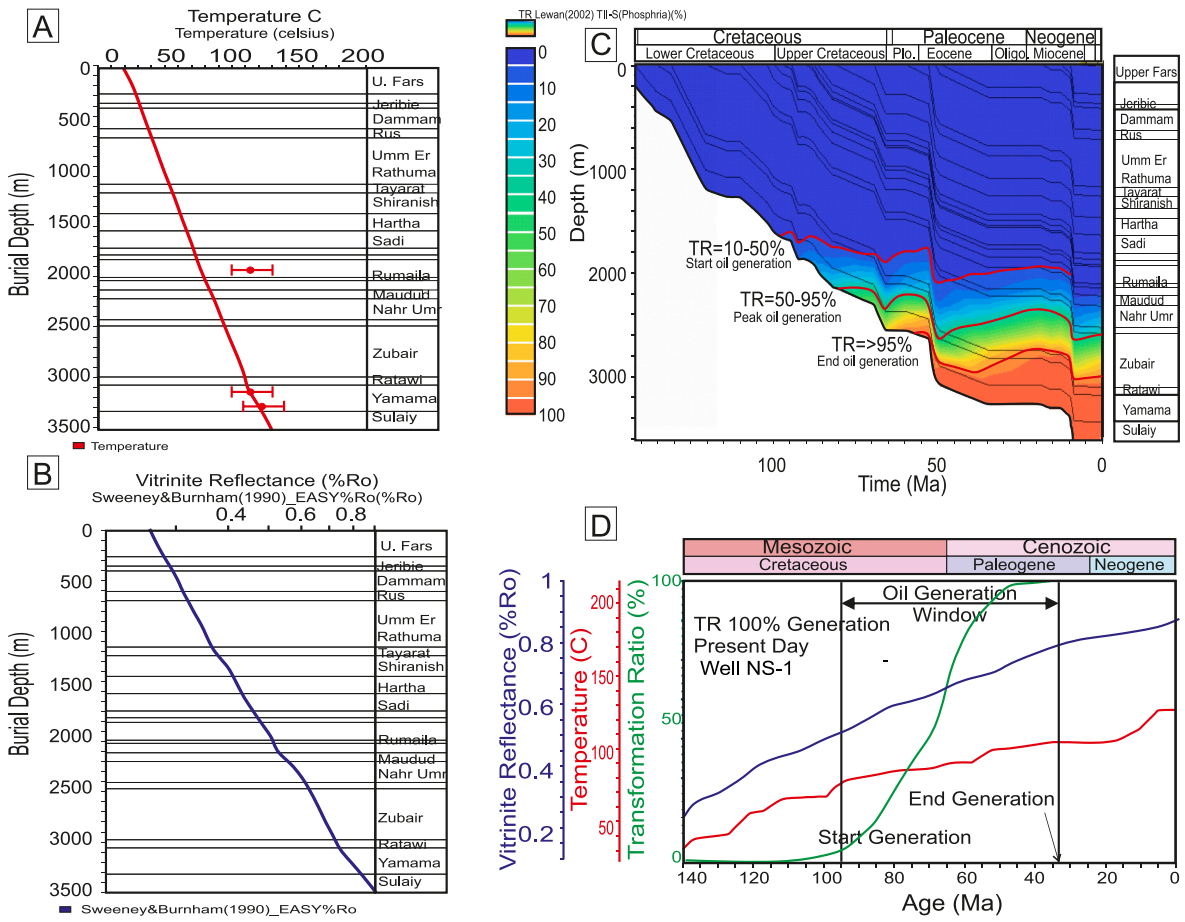

Fig. 20. A; A: The temperature utilized to estimate the best fit of the NS-1 well's current heat flow. B: Model calibration is achieved by comparing Sweeney's and Burnham's measured and modeled vitrinite reflectance. C: The NS-1 well's burial thermal history model. D: Thermal maturation of organic materials from the Yamama Formation's source interval in the NS-1 well over geological time.

horizontally as the depositional environment, the quality of kerogen, and the extent of its thermal maturity varied vertically within the same well and horizontally throughout the study area, as shown in Fig. 22A and B.

The geochemical analysis of the samples revealed that the kerogen in the organic-rich intervals of the Suba and Nahr Umr oil fields is of type I, which generates oil. Type II oil-pron kerogen can also be found in the oil fields of Rumaila, Nahr Umr, Suba, and Zubair, while type II/III kerogen can be found in the oil fields of West Qurna, North Rumaila, and Majnoon. Gas-pron kerogen of type III has been observed in the Jreshan oil field, as well as in some samples from the Luhais and Tuba. Except for a few samples taken from the higher sections of the formation in the Suba, Nahr Umr, Ratawi, Jreshan, and Luhais oil fields, the majority of the samples were thermally mature.

The majority of samples taken from wells located west of the study area, or on the inner shelf of (Sadooni, 1993), contain kerogen of the III types, which generates gas, whereas the majority of samples taken east of the study area, or on the outer shelf, contain kerogen of the II or II/III type, which generates oil. However, there is no clear association between the distribution of the Yamama formation's horizontal stratigraphic facies and the quality and thermal maturity of kerogen. Although thermal maturation increases to the east (Ibrahim، 1984), it is also influenced by kerogen quality and depth. The Nahr Umr-7 well samples contain all types of kerogens at varying depths. A kerogen type II sample from NR-9 at depth 3393 m, for example, had a Tmax of 440 °C, while a kerogen type III sample from depth 3566 had a Tmax of 434 °C. Fig. 22-B illustrates a cross section of a stratigraphic column of chosen wells along the study area from east to west, displaying the depths of the Yamama formation and its horizontal extension, as shown on the map in Fig. 22-A.

6. Conclusions

The Yamama formation is significant because it comprises significant reservoir units in central and southern Iraq, as well as the presence of source rock intervals at the same time. The significance of this study stems from the fact that it is the first geochemical study that covers the majority of the fields in central and southern Iraq. The examination of palynofacies, pyrolysis, biomarkers, and carbon isotopes revealed that the Yamama Formation source intervals had a high hydrocarbon efficiency and were deposited in a suboxic to anoxic marine environment that varied with the presence of some continental deposits. The TOC content was up to 5.12 wt% and the petroleum potential (S1+S2) was up to 28.65, which means that the Yamama source intervals varied from poor to excellent. Sedimentary organic matter kerogen types differ from the I, II, II/III, and III that yield oil and gas. Thermal maturity ranges from early maturation to peak maturity, and numerous samples have been recorded as thermally immature in some study wells. Models of the burial history and thermal maturity revealed that the formation was generated and expelled the oil, which migrated to neighboring reservoirs. The source intervals in the Nasiriyah oilfield began oil generation (% TR) in the Late Cretaceous (ca. 90 Ma ago) and ended oil generation (TR > 95%) in the Late Eocene (ca. 36 Ma ago), and these sources in other investigated oil fields started generating oil to the present day. Previous studies, such as (Al-Khafaji et al., 2019a), have indicated that the oil contained in many reservoir units of the formation is derived

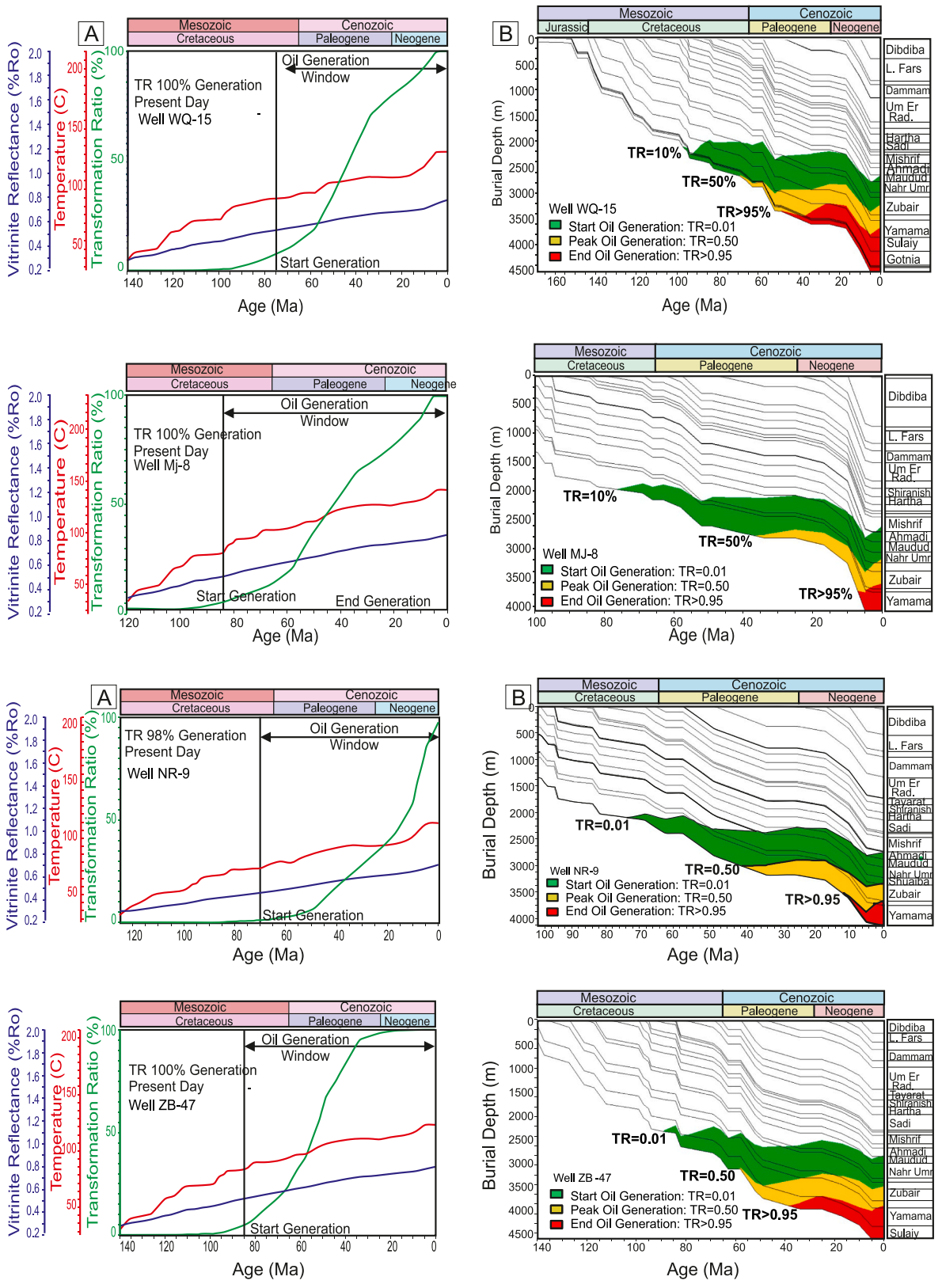

Fig. 21. A: Thermal maturation of Yamama Formation organic matter over geological time, and B: Burial thermal history model, in WQ-15, MJ-8, NR-9, and ZB-47 wells.

directly from the Yamama source rocks themselves.

Credit author statement

Amer Jassim Al-Khafaji: Conceptualization, Methodology, Writing – original draft preparation; **Fahad M. Al-Najm.**: Software,

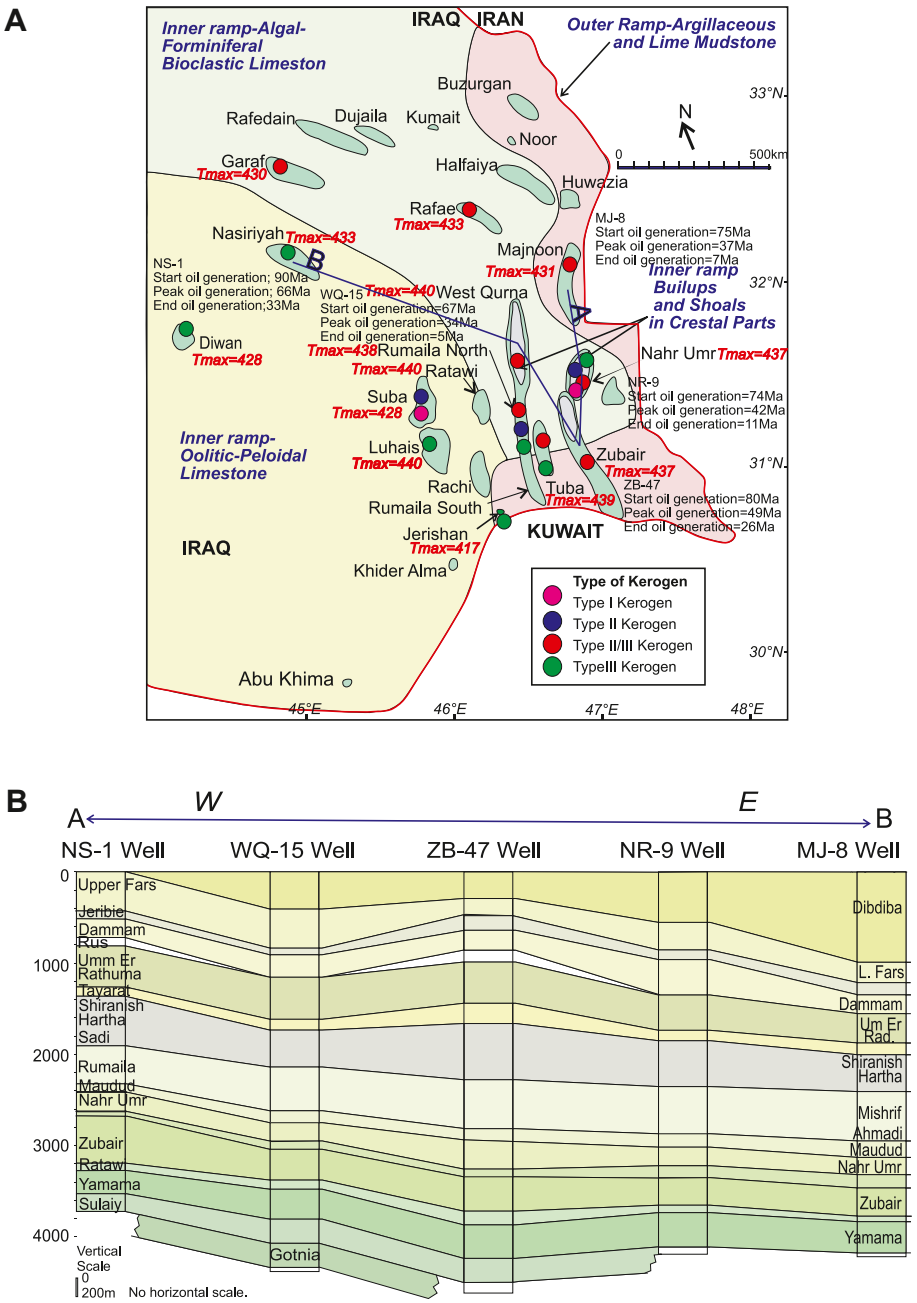

Fig. 22. A. A map of the locations of the Yamama formation samples, showing the quality of kerogen and its thermal maturity throughout the study area, and the timing of oil generation. Fig. 22-B. A cross section between A and B (see Fig. 5A) illustrates a correlation of the stratigraphic sequences of selected wells from the oil fields along the area of study, as well as formation depths and thicknesses, as well as the depths and extensions of the Yamama Formation.

Investigation, Data curation, **Rana A. K. Al-Refaia**: Visualization, Investigation.; **Fadhil N. Sadooni**: Supervision., Writing- Reviewing and Editing, **Mohanad R. A. Al-Owaidi**: Software, Validation; **Hamid A. Al-Sultan**: Writing- Reviewing and Editing.

Declaration of competing interest

The authors declare that they have no known competing financial interests or personal relationships that could have appeared to influence the work reported in this paper.

Acknowledgment

The authors would like to thank the *Basra Oil Company* in Basra and the Iraqi *Oil Exploration Company* in Baghdad for supplying the samples and data for the study, as well as their ongoing collaboration and assistance. We would also like to thank *GeoMark Research* in the United States for undertaking the geochemical analyses of the samples.

References

Abeed, Q., Al-Khafaji, A.J., Littke, R., 2011. Source rock potential of the upper jurassic lower cretaceous succession in the southern part of the Mesopotamian Basin (Zubair subzone), southern Iraq. J. Petroleum Geosci. 34 (2), 117–134.

Abeed, Q., Littke, R., Strozyk, F., Uffmann, A.Q., 2013. The Upper Jurassic–Cretaceous petroleum system of southern Iraq: a 3-D basin modelling study. GeoArabia ume 18, 179–200.

Ahmed, A.A.A., Al Obaidi, Q.A., 2018. Geochemical characteristics and modeling of conventional petroleum system of Majnoon oil field, south Iraq. Al-Nahrain J. Sci. 19 (4), 48–65.

Al-Ameri, T.K., Ai-Khafaji, A.J., 2014. a. Oil seep affinity and basin modeling used for hydrocarbon discoveries in the Kifle, Merjan, and Ekheither fields, West Iraq. Arabian J. Geosci. 7 (8), 273–5294.
Al-Ameri, T.K., Al-Khafaji, A.J., Zumberge, J., 2009. Petroleum system analysis of the Mishrif reservoir in Ratawi, Zubair, north and south Rumaila oil fields, southern Iraq. GeoArabia ume 14, 91–108.
Al-Ameri, T.K., et al., 2011. Programed oil generation of the Zubair Formation, Southern Iraq oil fields: results from PetroMod software modeling and geochemical analysis. Arabian J. Geosci. ume 4, 1239–1259.
Al-Khafaji, A., Najm, Al, , F. M., Ibrahim, Al, , R. N., Sadooni, F.N., 2019a. Geochemical investigation of Yamama crude oils and their inferred source rocks in the Mesopotamian Basin, Southern Iraq. Petrol. Sci. Technol. 37 (18), 25–2033.
Al-Khafaji, A., Hakimi, M.H., Najaf, A.A., 2018. Organic geochemistry characterization of crude oils from Mishrif reservoir rocks in the Southern Mesopotamian basin, South Iraq: implication for source input and paleoenvironmental conditions. Egypt. J. Petrol. 27 (1), 117–130.
Al-Khafaji, A.J., et al., 2021b. Geochemical characterization and origin of the Cretaceous Sa'di, Khasib, Mishrif, and Nahr Umr Crude Oils in Halfaya Oilfield, Southern Mesopotamian Basin, Iraq. Petrol. Sci. Technol. 39 (21–22), 993–1007.
Al-Khafaji, A.J., 2015. The Mishrif, Yamama, and Nahr Umr reservoirs petroleum system analysis, nasiriya oilfield, southern Iraq. Arabian J. Geosci. 8 (2), 81–798.
Al-Khafaji, A.J., et al., 2020. Organic geochemistry of oil seeps from the Abu-Jir Fault Zone in the Al-Anbar Governorate, western Iraq: implications for early-mature sulfur -rich source rock. Petrol. Sci. Eng. ume 184, 106584.
Al-Khafaji, A.J., et al., 2021. Geochemical characteristics of crude oils and basin modelling of the probable source rocks in the Southern Mesopotamian Basin, South Iraq. J. Petrol. Sci. Eng. ume 196, 107641.
Al-Khafaji, A.J., Sadooni, F., Hindi, M.H., 2019b. Contribution of the Zubair source rocks to the generation and expulsion of oil to the reservoirs of the Mesopotamian Basin, Southern Iraq. Petrol. Sci. Technol. 37 (8).
Al-Marsoumi, A.M., Abdul-Wahab, D., Al-Mohamed, R.A., 2005. Evaluation of organic matter in the Yamama formation at West Qurna oil field, southern Iraq. Iraqi Jour. Earth Sci. 5 (1), 9–17.
Al-Siddiki, A.A., 1978. Subsurface stratigraphy of southern Iraq. In: Proceedings. Libya, s.n.
Aqrawi, A.A., Badics, B., 2015. Geochemical characterisation, volumetric assessment and shale-oil/gas potential of the Middle Jurassic–Lower Cretaceous source rocks of NE Arabian Plate. GeoArabia 20 (3), 99–140.
Aqrawi, A., Goff, J.C., Horbury, A.D., Sadooni, F.N., 2010. The Petroleum Geology of Iraq. Beaconsfield, United Kingdom: Scientific Press Ltd, PO Box 21, Beaconsfield, Bucks, HP9 1NS.
Beydoun, Z., Hughes Clark, M.W., Stoneley, R., 1992. In: Macqueen, R.W., Leckie, D.A. (Eds.), Petroleum in the Mesopotamian Basin: A Late Tertiary Foreland Basin Overprinted onto the Outer Edge of a Vast Hydrocarbon-Rich Paleozoic-Mesozoic Passive-Margin Shelf.. Foreland Basins and Fold Belts, pp. 309–339. Volume Memoir 55.
Buday, T., Jassim, S.Z., 1984. Tectonic Map of Iraq, 1: 1000 000, scale Series, sheet No.2, Tectonic Map of Iraq. Publication of GEOSURV, Baghdad, Iraq.
Burrus, J., Audebert, F., 1990. Thermal and compaction processes in a young rifted basin containing evaporites, Gulf of Lions, France. Am. Assoc. Petrol. Geol. ume 74, 1420–1440.
Chafeet, H., Nawfal, N.A., Handhal, A.M., 2020. Palynofacies and source rocks evaluation for selected samples of subba oil field, southern Iraq. Iraqi J. Sci. 61 (5), 1063–1079.
Didyk, B.M., Simoneit, B.R., Brassell, S.C., Eglinton, G., 1978. Organic geochemical indicators of palaeoenvironmental conditions of sedimentation. Nature ume 272, 216–222.
Ibrahim, M., 1984. Geothermal gradients and geothermal oil generation in Southern Iraq. A preliminary investigation. J. Petrol. Geol. 7 (1), 77–86.
Peter, K.E., Cliford, C.W., Moldowan, J.M., 2005. *The biomarker Guide, Volume 2–Biomarkers and Isotopes in Petroleum Exploration and Earth History*. UK. Cambridge University Press.
Peters, K.E., 1986. Guidelines for evaluating petroleum source rock using programmed pyrolysis. American. Am. Assoc. Petrol. Geol. Bull. ume 87.
Pitman, J.K., Steinshouer, D., Reiser, H., Lewan, M.D., 2004. Petroleum generation and migration in the Mesopotamian Basin and Zagros fold belt of Iraq: results from a basin-modeling study. GeoArabia 9 (4), 41–72.
Sadooni, F., 1993. Tratigraphic sequence, microfacies, and petroleum prospects of the Yamama formation, lower cretaceous, southern Iraq. AAPG ume 77, 1971–1988.
Sadooni, F.N., 2018. Stratigraphy and lithologic characterization of the jurassic-cretaceous boundary across the Arabian Plate. Geneva, Switzerland, s.n. 70–71.
Sadooni, F.N., 2010. Impact of Growing Structures on Carbonate Facies Differentiation: an Example from the Yamama Formation in West Qurna Field, Southern Iraq. The Geological Society, London, pp. 1–2 s.l.
Sharland, R., et al., 2011. Arabian Plate Sequence Stratigraphy. Geo Arabia Special Publication, Gulf Petro link, Bahrain. Manama.
Sofer, Z., 1984. Stable carbon isotope compositions of crude oils: application to source depositional environments and petroleum alteration. AAPG (Am. Assoc. Pet. Geol.) Bull. ume 68.
Staplin, F.L., 1969. Sedimentary organic matter. organic inetramorphism, and oil and gasocairrence. Bull. Cavaclion Petrol. Geol. ume 17, 47–66.
Steinke, A., Bramkamp, R.A., 1952. Mesozoic rocks of eastern Saudi Arabia. AAPG Bull. 36, 900.
Tissot, B.P., Welte, D.H., 1984. Petroleum Formation and Occurrence. A New Approach to Oil and Gas exploration. Springer Verlag, Berlin.
Tyson, R.V., 1995. Sedimentary Organic Matter, Organic Facies and Palynofacies. s.l.: Springer, Dordrecht.
Waples, D.W., 1988. Time and temperature in petroleum formation: application of Lopatin's method to petroleum exploration. AAPG (Am. Assoc. Pet. Geol.) Bull. ume 64, 916–926.
Zumberge, J.E., Russell, J.A., Reid, S.A., 2005. Charging of Elk Hills reservoirs as determined by oil geochemistry. APG Bull. 89 (10), 1347–1371.